Innovative in situ remediation of mine waters using a layered double hydroxide-biochar composite

Veronika Veselská, Hana Šillerová, Barbora Hudcová, Gildas Ratié, Petr Lacina, Bronislava Lalinská-Voleková, Lukáš Trakal, Peter Šottník, Ľubomír Jurkovič, Michael Pohořelý, et al.

Journal Pre-proof

Innovative in situ remediation of mine waters using a layered double hydroxide-biochar composite

Veronika Veselská, Hana Šillerová, Barbora Hudcová, Gildas Ratié, Petr Lacina, Bronislava Lalinská-Voleková, Lukáš Trakal, Peter Šottník, Ľubomír Jurkovič, Michael Pohořelý, Delphine Vantelon, Ivo Šafařík, Michael Komárek

Please cite this article as: Veronika Veselská, Hana Šillerová, Barbora Hudcová, Gildas Ratié, Petr Lacina, Bronislava Lalinská-Voleková, Lukáš Trakal, Peter Šottník, Ľubomír Jurkovič, Michael Pohořelý, Delphine Vantelon, Ivo Šafařík and Michael Komárek, Innovative in situ remediation of mine waters using a layered double hydroxide-biochar composite, *Journal of Hazardous Materials,* (2021) doi:https://doi.org/10.1016/j.jhazmat.2021.127136

This is a PDF file of an article that has undergone enhancements after acceptance, such as the addition of a cover page and metadata, and formatting for readability, but it is not yet the definitive version of record. This version will undergo additional copyediting, typesetting and review before it is published in its final form, but we are providing this version to give early visibility of the article. Please note that, during the production process, errors may be discovered which could affect the content, and all legal disclaimers that apply to the journal pertain.

Innovative in situ remediation of mine waters using a layered double hydroxide-biochar composite

Veronika Veselská[a][1]*, Hana Šillerová[a], Barbora Hudcová[a], Gildas Ratié[a,b], Petr Lacina[c],
Bronislava Lalinská-Voleková[d], Lukáš Trakal[a], Peter Šottník[e], Ľubomír Jurkovič[f], Michael
Pohořelý[g,h], Delphine Vantelon[i], Ivo Šafařík[j,k], Michael Komárek[a]

[a] Department of Environmental Geosciences, Faculty of Environmental Sciences, Czech University of Life
Sciences Prague, Kamýcka 129, 165 00 Prague-Suchdol, Czech Republic

[b] Univ. Orléans, CNRS, BRGM, ISTO, UMR 7327, F-45071, Orléans, France

[c] GEOtest, a.s., Šmahova 1244/112, 627 00 Brno, Czech Republic

[d] Slovak National Museum, Vajanského nábrežie 2, 810 06 Bratislava, Slovakia

[e] Department of Mineralogy, Petrology and Mineral Deposits, Faculty of Natural Sciences, Comenius University
in Bratislava, Mlynská dolina, Ilkovicova 6, 842 15 Bratislava, Slovakia

[f] Department of Geochemistry, Faculty of Natural Sciences, Comenius University in Bratislava, Mlynská dolina,
Ilkovicova 6, 842 15 Bratislava, Slovakia

[g] Institute of Chemical Process Fundamentals of the Czech Academy of Sciences, v. v. i., Rozvojová 135, 165 02
Prague-Suchdol, Czech Republic

[h] Department of Power Engineering, Faculty of Environmental Technology, University of Chemistry and
Technology Prague, Technická 5, 166 28 Prague 6, Czech Republic

[i] SOLEIL synchrotron, L'orme des merisiers, Saint Aubin BP48, 91192 Gif-sur-Yvette Cedex, France

[j] Department of Nanobiotechnology, Biology Centre, ISB, CAS, Na Sádkách 7, 370 05 České Budějovice, Czech
Republic

[k] Regional Centre of Advanced Technologies and Materials, Czech Advanced Technology and Research
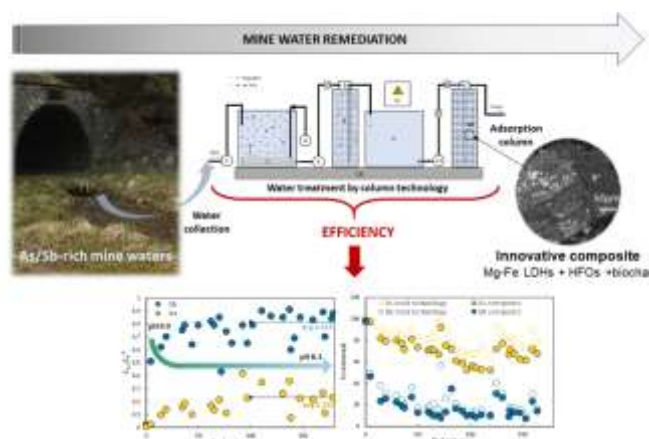Institute, Palacky University, Šlechtitelu 27, 783 71 Olomouc, Czech Republic

* corresponding author; email: veronika.veselska@upol.cz

---

[1] Present address: Regional Centre of Advanced Technologies and Materials, Czech Advanced Technology and
Research Institute, Palacký University Olomouc, Šlechtitelu 27, 783 71 Olomouc, Czech Republic

Abstract

The current demand for alternative water sources requires the incorporation of low-cost composites in remediation technologies; these represent a sustainable alternative to more expensive, commercially used adsorbents. The main objective of this comprehensive field-scale study was to incorporate the layered double hydroxides (LDHs) into the hybrid biochar-based composites and apply an innovative material to remediate As/Sb-rich mine waters. The presence of hydrous Fe oxides (HFOs) within the composite enhanced the total adsorption efficiency of the composite for As(V) and Sb(V). The kinetic data fitted to a pseudo-second order model. Equilibrium experiments confirmed that the composite had a stronger interaction with As(V) than with Sb(V). The efficient removal of As(V) from mine water was achieved in both batch and continuous flow column systems, reaching up to 98% and 80%, respectively. Sb(V) showed different behavior to As(V) during mine water treatment, reaching adsorption efficiencies of up to 39% and 26% in batch and column experiments, respectively. The migration of Sb(V) in mine water was mostly attributed to its dispersion before it was able to show affinity to the composite. In general, the proposed column technology is suitable for the field remediation of small volumes of contaminated water, and thus has significant commercial potential.

Graphical abstract

Keywords:

1. Introduction

Currently, more and more areas are facing water shortages due to excessive demands, climate change, and the contamination of water resources [1-3]. Simultaneously, there is a pressing need for new cost-effective water treatment methods that promote the involvement of readily available materials in remediation technologies. As biochar has been proven to be an efficient biomaterial regarding the removal of organic and inorganic substances from water, biochar-based technologies are becoming a promising tool within water remediation measures [4-8]. The limited removal efficiency of pristine biochar for anions can be enhanced by surface modification using various minerals, reductants, organic compounds, or nanoparticles through their fixation on the surface of biochar or trapping inside its pores. [9-15].

One of the possible minerals suitable for biochar modification are synthetic layered double hydroxides (LDHs). They are becoming increasingly important as they have been recently widely used in biomedicine, electrochemistry, catalysis, materials and polymer chemistry, or environmental remediation [16, 17]. The main mechanisms governing the retention of metals and metalloids via LDHs (complexation, electrostatic interactions, reduction, and surface precipitation) depend on their large specific surface area and stability, positive surface charge and high anion sorption efficiency [18-25]. To improve selective removal of metal cations from contaminated waters, modification of LDHs with different intercalated anions (CO_3^{2-}, NO_3^-, S_5^{2-} and MoS_4^{2-}) as efficient binding sites for metals has been performed over a broad pH range. Metals could be adsorbed either as various coordinated complexes in LDHs interlayer region or precipitated on surface as hydroxides or carbonates [26-28]. Moreover,

LDHs layers offer protective space for intercalated anions against oxidation so they can work well as regulating redox centers [29, 30].

For application of LDHs in water remediation processes, the presence of various ions is critical to control LDHs aggregation and to develop stable suspensions. Each specific anion affects the charging and colloidal stability of the LDHs. Stronger multivalent anion adsorption on the positively charged LDHs surface reduces more surface charge density, which amplifies the attractive van der Waals forces between LDHs particles. The electrophoretic mobility of LDHs decreases and their rapid aggregation leads to the colloidal instability of the LDHs suspension [31, 32]. Dilution of stable suspensions could also very effectively induce aggregate instability and the rapid sedimentation and separation of the LDHs, which facilitate its higher removal from contaminated water [33].

Nowadays, the challenge of producing cost-effective and sustainable composites needs to be urgently addressed. Hence incorporation of LDHs into the hybrid biochar-based composites is one of the ways to achieve either a better chemical stability of the LDHs or to synergize the adsorption of contaminants [34]. Efforts have been made to reduce LDHs production costs by incorporating boron mud/red mud or residual acidic solutions from the galvanizing process into their synthesis [35-37]. Possible applications of LDH-biochar composites include cleaning local water pollution, such as mine water from abandoned galleries and open adits. One of the greatest environmental concerns in former mining areas is the oxidative weathering of arsenopyrite (FeAsS) and stibnite (Sb_2S_3) [38-41], which can lead to pollution from the toxic oxyanions As(V) and Sb(III/V) in surface water and surrounding alluvial sediments. It has been proposed that the highly efficient adsorption of co-occurring As(V) and Sb(V) in mine waters could be achieved by modifying biochar's surface with ferric-based LDHs [42, 43]. Indeed, LDHs of different compositions have been successfully used to treat As-contaminated waters [18, 44-47].

This field scale study emphasized a unique approach by reusing cheap waste materials, i.e., readily available Fe-rich sludges, to produce a new, efficient, and innovative composite. Certified woody biochar modified by Mg-Fe LDHs, hereafter referred to as "composite," was prepared, tested, and applied to clean local As/Sb-rich outflows from open mine adits. The rates of As and Sb adsorption efficiency were determined to assess the benefits of using the prepared composite to remediate mine water. Furthermore, an improved LDHs synthesis by reusing waste materials could promote the preparation of multifunctional composites which is hopefully leading to their more efficient field applicability for As/Sb-rich mine water treatment.

2. Materials and Methods

2.1. Composite synthesis and characterization

Mg-Fe LDHs were prepared from Fe-rich sludges originating from previous black coal mining; they were collected from a hereditary adit (Oslavany, Czech Republic). Certified woody biochar NATURE CARBON (ENERGO Zlatá Olešnice s.r.o.) [48] was used as a carrier to precipitate Mg-Fe LDHs with hydrous Fe oxides (HFOs) during the synthesis of the composite (Table S1). The synthesis consisted of a modified co-precipitation protocol that has been previously described for pristine Mg-Fe LDHs with a molar Mg:Fe ratio of 4:1 [18, 49]. To obtain required Mg-Fe ratio, input Fe concentration was fixed by Fe-rich extract dilution prior each composite synthesis. Thus, Fe amount was known and reproducible for each synthesis and a normative procedure of Fe recovery from sludges is applicable even for composite synthesis on a larger scale in pilot plant conditions. Complete synthesis protocol is described in detail in SI. Subsequently, the composite was analyzed to determine the bulk

chemical composition; pH_{H_2O}, pH_{PZC}, cation exchange capacity (CEC), surface area (S_{BET}), volume of micropores (V_{micro}), mesopores surface area (S_{meso}), and total pore volume (V_{tot}) (Table 1). The mineralogical structure of the composite was determined by X-ray Diffraction (XRD; Bruker D8 Discover diffractometer). Scanning Electron Microscope (SEM) images and chemical compositions of mineral phases were obtained with a variable-pressure SEM (Tescan Vega 3XMU) that was equipped with an energy dispersive spectrometer (EDS; Bruker X'Flash 5010). After the contact with mine waters, the chemical composition of the composite was characterized with an electron probe microanalyzer (EMPA; CAMECA SX-100) equipped with four wavelength dispersive X-ray spectrometers (WDSs). The Fe solid speciation in the composite was determined by X-ray absorption spectroscopy (XAS) measurements at LUCIA beamline (SOLEIL Synchrotron, France) (Table S2) [50, 51]. Each methodological approach is provided in SI.

2.2. Sampling sites and mine water collection

Two specific localities, strongly impacted by Sb sulfides released from mining ore over the last two centuries in Slovakia, were selected to evaluate the composite efficiency (see SI). During 2018-2019, As and Sb rich drainage waters from adits and tailings ponds (sample 1), as well as mine water outflows from open adits (sample 2) were collected (Figure 1, Table S3). Considering the specific pH-Eh conditions of mine waters and in accord with previous studies, dissolved $[HAsO_4]^{2-}$ and $[Sb(OH)_6]^-$ were assumed to be mostly present [40, 52-54]. Therefore, the aqueous speciation of As and Sb was accepted to be As(V) and Sb(V), respectively, in this study. Moreover, mine waters with different Fe contents were collected for in situ composite application. Thus, the role of dissolved Fe in natural attenuation of contaminants was considered while evaluating the efficiency of the composite.

2.3. Batch experiments

Kinetic (i) and equilibrium (ii) batch experiments using synthetic solutions prepared from $(HAsNa_2O_4) \times 7\ H_2O$ and $KSb(OH)_6$, were performed to measure the total amounts of As(V) and Sb(V) adsorbed on the composite (i) at an initial concentration of 10^{-4} mol L^{-1} for both As(V) and Sb(V) with 1 g L^{-1} of composite in suspension (sampled at selected time intervals over days, see SI and Table S4, Figure S1-S2), and (ii) at different initial concentrations of As(V) and Sb(V) (50, 100, 150, 200, 250, and 500 mg L^{-1}) with 10 g L^{-1} of composite in suspension after reaching equilibrium (24 hours and 48 hours for As(V) and Sb(V), respectively; SI and Table S5 and Figure S3). Consequently, kinetic batch experiments were conducted with samples 1 and 2 to evaluate the adsorption efficiencies of the composite for As(V) and Sb(V) (SI).

2.4. Column experiments

Laboratory column experiments were set-up based on the optimization of parameters (flow rate, mass of composite, and column dimensions) to provide the most effective removal of As(V) and Sb(V) from mine waters in a flow-through system (Table S6). Dynamic flow adsorption testing was conducted at small and large scales (SI and Figure 2a) to monitor the adsorption efficiency of the composite and test the final arrangement for column technology intended for its field application. The slight differences in parameters (Table 2) resulted from changes made due to actual technical possibilities or limitations. The pH, Eh, conductivity, and temperature were determined periodically for the mine water from the supply tank, after

aeration, after filtration, and after treatment (Table S7-S10). The elemental concentrations were analyzed by ICP-OES and ICP-MS.

2.5. Field application

The composite was field-tested using a mobile double-column technology combining three technological operations: aeration, filtration, and adsorption (see SI for details, Figure 2b-c). In general, outflows of mine water were continuously pumped into the aeration tank and filtration column filled with filter quartz sand to remove undissolved particles or precipitated Fe oxyhydroxides. Pre-treated mine water was injected into the adsorption column (AC) filled with a mixture of quartz sand and the composite in an optimal mass ratio of 15:1, according to the laboratory experiments. The treated effluent, untreated inlet mine water, mine water from the aeration tank, and effluents from the filtration column were sampled regularly after 100 to 200 liters had flowed through the column device. For collected samples, pH, Eh, conductivity, temperature, and the concentrations of elements were measured as previously described (Tables S11-S12). The concentration data from the continuous flow column experiments were evaluated using breakthrough curves (BTCs).

The total adsorption efficiencies of the column technology for As(V) and Sb(V) (%) were calculated from the total treated volume of mine water. The AC capacity, q_j (mg g^{-1}), was calculated as:

$$q_j = \frac{c_j^f Q}{1000 m_s} \int_0^t \left(1 - \frac{c_j^{out}}{c_j^f} \right) dt \qquad \text{(Eq. 1)}$$

where q_j is the concentration of metal j in the adsorbent (mg g^{-1}), c_j^f is the feeding concentration of j in the mine water (mg L^{-1}), Q is the flow rate through the column (mL min$^-$

[1]), m_s is the mass of material in the column (g), c_j^{out} is the outlet concentration of j in the mine water (mg L^{-1}), and t is the time at which the feeding concentration of j is equal to 95% of its outlet concentration [55]. The integral term of Eq. (1) was calculated through numerical integration using the ORIGIN 2020 software.

3. Results and Discussion

3.1. Composite characterization

One of the main challenges in precipitating Mg-Fe LDHs during the composite synthesis is ensuring the reusability of Fe sludges to minimize the use of chemical reagents. The phase identification of the composite revealed that it had a low degree of crystallinity. Only two broad peaks with low intensity were detected at values of 2Θ (approximately 11.42 and 22.87; these values were typical for pristine 4:1 Mg-Fe LDHs as previously reported by Hudcová et al. [18]. Additional characterization by SEM/EDS highlighted the heterogeneous distribution of Mg-Fe LDHs on the biochar surface and high Fe content in the newly formed precipitates (27.80 wt% of Fe on average, Figure 3a, b, Table S13). Indeed, the observed high Fe concentrations indicated the additional precipitation of intermediate amorphous Fe-rich products. The linear combination fits performed on the Fe XANES spectra confirmed that 31% and 69% of the total Fe in the composite was related to pristine Mg-Fe LDHs and HFOs, respectively Similar results were confirmed for Mg-Fe LDHs with 39% and 61% of the total Fe related to pristine Mg-Fe LDHs and HFOs, respectively (Figure 3c, Table S2). This observation agreed with the findings of Jaśkaniec et al. [56]. It supports the precipitation of thermodynamically metastable Fe oxyhydroxides during the synthesis of LDHs at room temperature, since reusing low-cost waste materials decrease the purity of intended LDHs.

Therefore, the composite represented a mixture of Mg-Fe LDHs, HFOs, and biochar, where each phase might have had a positive effect on the adsorption of As(V) and Sb(V) [6, 18, 47, 57, 58]. As HFOs have been recognized to strongly sequestrate As(V) and Sb(V) agents in the environment, their presence likely favored the enhancement of the total adsorption efficiency of the composite. The determination of As(V) and Sb(V) speciation in the interactions with the different phases of the composite will require more sensitive methods, including nano-XRF mapping and μXANES; this needs to be considered for future studies.

3.2. As(V) and Sb(V) removal from mine waters

The rate of simultaneous removal of As(V) and Sb(V), their different initial concentrations, and their competitive behaviors were considered under the specific Eh-pH conditions of mine water samples (Table S3). The As(V) adsorption rate increased with decreasing initial As(V) concentrations in mine water samples. Based on equilibrium batch experiments, the As(V) adsorption data were sufficiently described by the L-class Freundlich isotherms ($R^2 > 0.956$, Table S5, Figure S3), which points to multilayered As(V) adsorption controlled by the heterogeneous adsorption sites with different free energies of sorption [59, 60]. The intensity of adsorption ($n < 1$) revealed that As(V) adsorption became less favorable with increasing amounts of As on the surface of the composite; which is in agreement with the adsorption kinetic experiments with mine waters. It can be stated that the rate of As(V) removal by the composite at high As concentrations might have been limited by (i) the number of free active sites on the surface of the composite and (ii) the competitive adsorption between As(V) and Sb(V) [42, 54, 61, 62]. Both, the As(V) and Sb(V) kinetic models best fitted a pseudo-second order reaction model (Table S4, Figure S1-S2). This indicates an inclination towards chemisorption as adsorption was the rate limiting step on the composite [63]. Indeed, surface

complexation has been previously shown to be one of the main anion-sorption mechanisms for both LDHs and LDH-biochar composites [18, 25, 47, 64-66]. Inner-sphere complexes have also been indicated between As(V)/Sb(V) and HFOs [67-69]. Since the Langmuir model fitted better the adsorption data for Sb(V) ($R^2 > 0.954$) than the Freundlich model, the surface of the composite is assumed to contain homogenous adsorption sites with equal affinity for Sb(V) [60, 70, 71].

A slightly higher maximum sorption capacity was determined for Sb(V) ($Q_{max} = 24.99$ mg g^{-1}) in comparison with As(V) ($Q_{max} = 20.98$ mg g^{-1}). Despite the difference in sorption capacity is not very significant, it revealed that longer contact time within equilibrium experiments plays an important role in the Sb(V) behavior (see SI). Slow, and long-term increasing trend in Sb(V) adsorption pointed out that Sb(V) needs more time to achieve the complete surface saturation. If vacant sites for adsorption on the surface of composite are still available, the adsorbate will be adsorbed more showing higher Q_{max} values. Despite magnetic and Fe-loaded biochars have demonstrated a promising capacity to adsorb As(V) in mine waters, wastewaters, and neutral drainages through electrostatic interactions and specific adsorption onto Fe-loaded particles [72-74], the presented composite appeared to be able to adsorb more As(V) than previously reported LDH-modified biochar [25, 65, 66] and Fe-impregnated biochar [75 - 79] (Table 3).

3.3. Adsorption efficiency of the composite

The composite demonstrated higher affinity of binding sites for As(V) ($b = 0.375$) as compared to Sb(V) ($b = 0.017$) via fitting by the Langmuir isotherm model and thus indicated a better selectivity for As(V) in comparison with Sb(V). This was also reflected in the high efficiency of the adsorption kinetic for As(V), achieving the adsorption of 96% and 98% of

10

total As(V) in 24 hours for samples 1 and 2, respectively. Ninety percent of As(V) was already adsorbed in the first ten minutes for sample 2, which reached a plateau of 98% in two hours. Contrary to As(V), only 34% of the total Sb(V) was adsorbed in 24 hours in sample 1. A similar 39% was observed for Sb(V) in sample 2, even where the Sb(V) concentration exceeded that of As(V).

In general, the Eh-pH conditions of treated mine water (see SI) control both the As(V) and Sb(V) speciation, their mobility and attenuation and the surface charge of the composite. While pH of mine water could indirectly affect the speciation of As by regulating the saturation indices of dissolved Fe, Eh controls the adsorption of both As(V) and Sb(V) [80]. Based on results reported in the published literature, the adsorption of oxyanions including As(V) by LDHs or by various biochar-based composites tends to decrease with increasing pH, especially at pH above 6, while competing with OH$^-$ for adsorption positions. Moreover, due to the instability of the LDHs structures at very low pH, the oxyanions adsorption could be decreased as well [43, 44, 45, 81]. Consistence efficiency of LDH-based materials or nanostructured composites for Sb(V) in a range of pH from 3 to 10 indicates a lower pH-dependency of Sb(V) adsorption [42, 82]. Unlike most of the studied adsorbents, unusually high pH$_{PZC}$ (10) of the composite presented in this study allows to maintain the surface of the composite positively charged over a broad range of pH values. Thus, physical adsorption of dissolved $[HAsO_4]^{2-}$ and $[Sb(OH)_6]^-$ under restricted pH (7-8) of treated mine water can be promoted due to the favorable electrostatic interactions [28, 42].

Interferences of As(V) and Sb(V) with other aqueous species need to be also considered. The natural pH of mine water and the buffering effect of Mg-Fe LDHs promoted the precipitation of carbonates onto the composite surface (Table S14-S15). Carbonate showed little effect on the sorption of Sb(V) [83], though the mobility of As(V) and Sb(V) can be slightly decreased via sequestration with carbonate minerals [84, 85]. However, the results of

XRD and EMPA show neither As(V) or Sb(V) adsorption on carbonates nor formation of calcium arsenates and calcium-antimony phases.

Batch experiments conducted for 160 days have confirmed the improvement of composite efficiency toward Sb(V) via extending the time of the interaction with mine water (Figure S4). Besides, while maintaining the same conditions of kinetic experiments, the composite presented higher As(V) and Sb(V) adsorption efficiency than pristine woody biochar used for composite synthesis. Additionally, adsorption efficiency of the composite was compared within this work with woody biochar coated by Fe- oxides or amorphous Mn- oxides, nanostructured carbon, or commercially used granulated active carbon (Figure 4). Composite showed better efficiency, which makes it more efficient material for further field applications in mine water remediation.

3.4. Post-cleaning of mine water

3.4.1. BTCs: laboratory and field scale column experiments

Efficient As(V) removal by the composite was afforded in the primary stages of the experiments, followed by the gradual growth of the BTCs (Figure 5). In the case of Sb(V), two-phase, asymmetric BTCs were observed at both laboratory and field scales. A rapid initial rise of $c_{OUT}\,c_0^{-1}$ was followed by very gradual growth till the feed concentration. In general, no significant differences were observed in the shapes and gradients of BTCs taken from small- and large-scale laboratory experiments, and within the field application. As depicted in Figure 5, about 200-300 bed volumes passed through the column on all three scales during column experiments. A complete saturation of the columns was reached for Sb(V) after ~230 - 300 bed volumes in sample 1 on laboratory scale. The columns could similarly treat ~ 220 bed volumes of Sb(V) within the field application before the saturation

point was achieved in sample 2. Based on treatable bed volumes, composite appears to be less efficient in comparison with biochar-supported $MnFe_2O_4$ magnetic nanocomposite or other nanostructured composites [81, 82]. However, the composite beds were not fully exhausted for As(V) and the binding sites did not become saturated at low As(V) inlet concentrations in mine water (mean 2.12 mg L^{-1} and 0.03 mg L^{-1} in samples 1 and 2, respectively). To obtain the complete concentration-volume profile for As(V), the experiments would need to be conducted for a much longer period and higher volume of mine water could have been treated.

When compared the treatable volumes for As(V) and Sb(V) at breakthrough point (c_{OUT} c_0^{-1} =0.5), thirty times higher bed volume for As(V) in comparison with Sb(V) reflects better performance of composite for As(V). This observation is consistent with the mutual effects observed in batch studies. The same similarity of adsorption results between batch and column experiments was also observed by Qiu et al. [86] via using a reusable granular TiO_2, providing evidence that both oxides and biochar-based composites with LDHs could be used for simultaneous removal of As(V) and Sb(V) from mining wastewater.

3.4.2. Adsorption efficiency of the technological column device

Column experiments performed on the composite revealed the adsorption of As(V) and Sb(V) under the actual environmental conditions of mine waters. The average contents of As, Sb, and Fe reached up to 2.12, 0.41, and 3.91 mg L^{-1}, respectively in sample 1 (pH 7.5) and 0.03, 1.05, and 0.05 mg L^{-1}, respectively in sample 2 (pH 7.7). In both cases, As and Sb concentrations exceeded the limits for surface waters according to the Regulation of the Government of the Slovak Republic No 269/2010 (0.0175 and 0.025 mg L^{-1} for As and Sb, respectively).

The adsorption efficiencies of the technological column device for As(V) and Sb(V) removal in the dynamic system were 80% and 26%, respectively, for sample 1. Here, the presence of free aqueous Fe (Table S11) led to the precipitation of fresh Fe oxyhydroxides, which can naturally reduce As(V) concentrations in mine water [54, 61]. Therefore, the arrangement of aeration and filtration within the column technology was essential for removing non-dissolved phases prior to the evaluation of the AC efficiencies (66% and 19% for As(V) and Sb(V), respectively). However, aeration and sand filtration in particular increased the total adsorption efficiency of the column device, though the proportion of scavenged As(V) within the filtration step was significantly higher than that of Sb(V) (Figure 6). The very low concentration of dissolved Fe in sample 2 (Table S12) means that the Sb(V) adsorption (25%) could be solely attributed to the AC processes.

In general, the adsorption of Sb(V) onto the composite was limited in the continuous flow setting. Moreover, q_i values, as determined from the BTCs, were 0.16 and 0.37 mg g^{-1} for samples 1 and 2, respectively. It is well known that flow rate is the most critical parameter that influences metalloid adsorption [87, 88]. Therefore, one of the reasons for the low column capacity could have been the influence of flow rate, which was approximately $75 - 92$ times higher (90-110 L hod^{-1}) than in the laboratory large scale experiments. Previous studies have confirmed that the presence and mobility of soluble Sb(V) oxyanions in mine water are preferably controlled by the kinetics of the formation of secondary Sb minerals [39]. Thus, Sb(V) migration in mine water is more attributable to dispersion as dissolved aqueous forms, rather than its affinity to suspended particulate matter, alluvial sediments, or HFOs deposited from discharged mine water [38, 89, 90]. Therefore, despite the natural attenuation of Sb(V) through either dilution or adsorption onto Fe oxyhydroxides [91, 92], the application of column technology with an effective composite provided an appropriate post-cleaning tool for mine water, prior to its draining into surface waters.

3.5. Engineering implications and benefits of the composite

This study aimed to examine the behavior of the composite in a fixed bed column and its performance when applied to mine water remediation. Consistent results between laboratory experiments and in situ application confirmed steady adsorption behavior of the composite for As(V) and Sb(V). Incorporating the composite into an engineered column device proved a promising, easy-to-operate, and efficient way to suitably complement passive mine water treatment, which is the current remedial strategy in Slovakia. To design a set of batch reactors in possible combination with column devices, it will be necessary to consider the impact of torrential rain, which can drastically increase mine water effluent yields. This could negatively affect the steady performance of the composite (Figure 5e). The benefits of the proposed column device include its flexible and ease of transport, which allow it to be used in less accessible places. The operative combination of aeration, filtration, and adsorption can be optimized regarding the type of treated water. For higher efficiency, the device allows the connection of two sorption columns in series mode. As the column device was designed for the controlled post cleaning of small volumes of water (approx. 1 m^3 per day), it could be useful also for ensuring water consumption in households or smaller businesses using treated water as an alternative source for irrigation or watering.

After the field application of the composite, the output concentrations of As(V) and Sb(V) in mine waters remained above the limits for surface waters stipulated by the Government Regulation of the Slovak Republic (Nr.269/2010). However, column device was able to successively produce about 14 bed volumes of clean water before being beyond the critical limit value of As for irrigation water (0.05 mg L^{-1}). Further studies will be required to maintain an efficiency over time.

The composites applied in mine water remediation are further considered as waste and should be collected, segregated, and safely disposed as per the environmental legislation available in a specific country. The treatment of contaminated composites in Slovakia is carried out in accordance with a valid waste disposal directive (Act No. 79/2015 Coll.). Due to the higher toxic substances content, there are two possible ways of composite handling: (i) landfilling as a hazardous waste with no previous treatment (if the content of selected contaminants is less than 1 wt%); (ii) processing and reusing it similarly to ferrous scrap at steel manufacturing plants. If appropriate, composite can be recommended for solidification with the aim of its further safe storage. In addition, composites provide economically important and viable Sb recovery sources, which is also in accordance with the strategic approach to accessing critical raw materials by the European Union.

4. Conclusions

The composite proposed in this study proved to be a consistent and innovative remediation tool for specific environmental loads such as mine water; it used on-site post-cleaning column technology designed particularly for the treatment of small volumes of local effluents. Following the idea of alternative Mg-Fe LDHs preparation, Fe-sludge was used to minimize production costs. The production of Mg-Fe LDHs was limited because of the precipitation of amorphous secondary Fe oxyhydroxides. However, their presence improved the composite's retention efficiencies for As(V) and Sb(V). Field experiments showed that the total efficiency of the mobile column technology was higher for As(V) than for Sb(V) regarding their removal from mine water (80-100% for As and 25-26% for Sb). The higher efficiency for As(V) resulted from the continuous flow settings and differences in behavior between As(V) and Sb(V), the latter was preferably controlled by the kinetics of the formation of secondary

Sb minerals. Further studies into the detailed aqueous speciation of Sb might help to further reveal this difference. The proposed technology can be easily transported and can also be used in less accessible locations.

Funding

Declaration of competing interest

The authors declare that they have no known competing financial interests or personal relationships that could have appeared to influence the work reported in this paper.

Acknowledgments

References

[1]   W. Brack, V. Dulio, M. Ågerstrand, I. Allan, R. Altenburger, M. Brinkmann, D. Bunke, R.M. Burgess, I. Cousins, B.I. Escher, F.J. Hernández, L.M. Hewitt, K. Hilscherová, J. Hollender, H. Hollert, R. Kase, B. Klauer, C. Lindim, D.L. Herráez, C. Miège, J. Munthe, S. O'Toole, L. Posthuma, H. Rüdel, R.B. Schäfer, M. Sengl, F. Smedes, D. van de Meent, P.J. van den Brink, J. van Gils, A.P. van Wezel, A.D. Vethaak, E. Vermeirssen, P.C. von der Ohe, B. Vrana, Towards the review of the European Union Water Framework Directive: Recommendations for more efficient assessment and management of chemical contamination in European surface water resources, Sci. Total Environ. 576 (2017) 720–737. https://doi.org/10.1016/j.scitotenv.2016.10.104.

[2]   Md.A. Abedin, A.E. Collins, U. Habiba, R. Shaw, Climate Change, Water Scarcity, and Health Adaptation in Southwestern Coastal Bangladesh, Int. J. Disaster Risk Sci. 10 (2019) 28–42. https://doi.org/10.1007/s13753-018-0211-8.

[3]   C. Payus, L. Ann Huey, F. Adnan, A. Besse Rimba, G. Mohan, S. Kumar Chapagain, G. Roder, A. Gasparatos, K. Fukushi, Impact of Extreme Drought Climate on Water Security in North Borneo: Case Study of Sabah, Water. 12 (2020) 1135. https://doi.org/10.3390/w12041135.

[4]   M. Ahmad, A.U. Rajapaksha, J.E. Lim, M. Zhang, N. Bolan, D. Mohan, M. Vithanage, S.S. Lee, Y.S. Ok, Biochar as a sorbent for contaminant management in soil and water: A review, Chemosphere. 99 (2014) 19–33. https://doi.org/10.1016/j.chemosphere.2013.10.071.

[5]   D. Mohan, A. Sarswat, Y.S. Ok, C.U. Pittman, Organic and inorganic contaminants removal from water with biochar, a renewable, low cost and sustainable adsorbent – A critical

review, Bioresour. Technol. 160 (2014) 191–202. https://doi.org/10.1016/j.biortech.2014.01.120.

[6] G. Ungureanu, S. Santos, R. Boaventura, C. Botelho, Arsenic and antimony in water and wastewater: Overview of removal techniques with special reference to latest advances in adsorption, J. Environ. Manage. 151 (2015) 326–342. https://doi.org/10.1016/j.jenvman.2014.12.051.

[7] W. Gwenzi, N. Chaukura, C. Noubactep, F.N.D. Mukome, Biochar-based water treatment systems as a potential low-cost and sustainable technology for clean water provision, J. Environ. Manage. 197 (2017) 732–749. https://doi.org/10.1016/j.jenvman.2017.03.087.

[8] L. Lu, W. Yu, Y. Wang, K. Zhang, X. Zhu, Y. Zhang, Y. Wu, H. Ullah, X. Xiao, B. Chen, Application of biochar-based materials in environmental remediation: from multi-level structures to specific devices, Biochar. 2 (2020) 1–31. https://doi.org/10.1007/s42773-020-00041-7.

[9] L. Trakal, R. Šigut, H. Šillerová, D. Faturíková, M. Komárek, Copper removal from aqueous solution using biochar: Effect of chemical activation, Arab. J. Chem. 7 (2014) 43–52. https://doi.org/10.1016/j.arabjc.2013.08.001.

[10] L. Trakal, V. Veselská, I. Šafařík, M. Vítková, S. Číhalová, M. Komárek, Lead and cadmium sorption mechanisms on magnetically modified biochars, Bioresour. Technol. 203 (2016) 318–324. https://doi.org/10.1016/j.biortech.2015.12.056.

[11] L. Trakal, Z. Michálková, L. Beesley, M. Vítková, P. Ouředníček, A.P. Barceló, V. Ettler, S. Číhalová, M. Komárek, AMOchar: Amorphous manganese oxide coating of biochar improves its efficiency at removing metal(loid)s from aqueous solutions, Sci. Total Environ. 625 (2018) 71–78. https://doi.org/10.1016/j.scitotenv.2017.12.267.

[12]   M.B. Ahmed, J.L. Zhou, H.H. Ngo, W. Guo, M. Chen, Progress in the preparation and application of modified biochar for improved contaminant removal from water and wastewater, Bioresour. Technol. 214 (2016) 836–851. https://doi.org/10.1016/j.biortech.2016.05.057.

[13]   X. Tan, Y. Liu, Y. Gu, Y. Xu, G. Zeng, X. Hu, S. Liu, X. Wang, S. Liu, J. Li, Biochar-based nano-composites for the decontamination of wastewater: A review, Bioresour. Technol. 212 (2016) 318–333. https://doi.org/10.1016/j.biortech.2016.04.093.

[14]   P. Ouředníček, B. Hudcová, L. Trakal, M. Pohořelý, M. Komárek, Synthesis of modified amorphous manganese oxide using low-cost sugars and biochars: Material characterization and metal(loid) sorption properties, Sci. Total Environ. 670 (2019) 1159–1169. https://doi.org/10.1016/j.scitotenv.2019.03.300.

[15]   M. Stefaniuk, P. Oleszczuk, Y.S. Ok, Review on nano zerovalent iron (nZVI): From synthesis to environmental applications, Chem. Eng. J. 287 (2016) 618–632. https://doi.org/10.1016/j.cej.2015.11.046.

[16]   M. Gräfe, K.G. Bunney, S. Cumberland, G. Douglas, Mechanisms of Uranyl Sequestration by Hydrotalcite, ACS Omega. 2 (2017) 7112–7119. https://doi.org/10.1021/acsomega.7b01050.

[17]   G. Varga, Z. Somosi, Z. Kónya, Á. Kukovecz, I. Pálinkó, I. Szilagyi, A colloid chemistry route for the preparation of hierarchically ordered mesoporous layered double hydroxides using surfactants as sacrificial templates, J. Colloid Interface Sci. 581 (2021) 928–938. https://doi.org/10.1016/j.jcis.2020.08.118.

[18]   B. Hudcová, V. Veselská, J. Filip, S. Číhalová, M. Komárek, Sorption mechanisms of arsenate on Mg-Fe layered double hydroxides: A combination of adsorption modeling and solid state analysis, Chemosphere. 168 (2017) 539–548. https://doi.org/10.1016/j.chemosphere.2016.11.031.

[19]   L. Trakal, D. Bingöl, M. Pohořelý, M. Hruška, M. Komárek, Geochemical and spectroscopic investigations of Cd and Pb sorption mechanisms on contrasting biochars: Engineering implications, Bioresour. Technol. 171 (2014) 442–451. https://doi.org/10.1016/j.biortech.2014.08.108.

[20]   Z. Wang, G. Liu, H. Zheng, F. Li, H.H. Ngo, W. Guo, C. Liu, L. Chen, B. Xing, Investigating the mechanisms of biochar's removal of lead from solution, Bioresour. Technol. 177 (2015) 308–317. https://doi.org/10.1016/j.biortech.2014.11.077.

[21]   T. Xie, K.R. Reddy, C. Wang, E. Yargicoglu, K. Spokas, Characteristics and Applications of Biochar for Environmental Remediation: A Review, Crit. Rev. Environ. Sci. Technol. 45 (2015) 939–969. https://doi.org/10.1080/10643389.2014.924180.

[22]   H. Li, X. Dong, E.B. da Silva, L.M. de Oliveira, Y. Chen, L.Q. Ma, Mechanisms of metal sorption by biochars: Biochar characteristics and modifications, Chemosphere. 178 (2017) 466–478. https://doi.org/10.1016/j.chemosphere.2017.03.072.

[23]   Y.-S. Ok, D.C.W. Tsang, N. Bolan, J.M. Novak, eds., Biochar from biomass and waste: fundamentals and applications, ELSEVIER, Amsterdam Oxford Cambridge, 2019.

[24]   P. Wu, S.T. Ata-Ul-Karim, B.P. Singh, H. Wang, T. Wu, C. Liu, G. Fang, D. Zhou, Y. Wang, W. Chen, A scientometric review of biochar research in the past 20 years (1998–2018), Biochar. 1 (2019) 23–43. https://doi.org/10.1007/s42773-019-00002-9.

[25]   X. Gao, Y. Peng, L. Guo, Q. Wang, C.-Y. Guan, F. Yang, Q. Chen, Arsenic adsorption on layered double hydroxides biochars and their amended red and calcareous soils, J. Environ. Manage. 271 (2020) 111045. https://doi.org/10.1016/j.jenvman.2020.111045.

[26]   A. Jawad, Z. Liao, Z. Zhou, A. Khan, T. Wang, J. Ifthikar, A. Shahzad, Z. Chen, Z. Chen, Fe-MoS4: An Effective and Stable LDH-Based Adsorbent for Selective Removal of Heavy Metals, ACS Appl. Mater. Interfaces. 9 (2017) 28451–28463. https://doi.org/10.1021/acsami.7b07208.

[27] A. Jawad, L. Peng, Z. Liao, Z. Zhou, A. Shahzad, J. Ifthikar, M. Zhao, Z. Chen, Z. Chen, Selective removal of heavy metals by hydrotalcites as adsorbents in diverse wastewater: Different intercalated anions with different mechanisms, J. Clean. Prod. 211 (2019) 1112–1126. https://doi.org/10.1016/j.jclepro.2018.11.234.

[28] J. Ali, H. Wang, J. Ifthikar, A. Khan, T. Wang, K. Zhan, A. Shahzad, Z. Chen, Z. Chen, Efficient, stable and selective adsorption of heavy metals by thio-functionalized layered double hydroxide in diverse types of water, Chem. Eng. J. 332 (2018) 387–397. https://doi.org/10.1016/j.cej.2017.09.080.

[29] J. Ali, L. Wenli, A. Shahzad, J. Ifthikar, G.G. Aregay, I.I. Shahib, Z. Elkhlifi, Z. Chen, Z. Chen, Regulating the redox centers of Fe through the enrichment of Mo moiety for persulfate activation: A new strategy to achieve maximum persulfate utilization efficiency, Water Res. 181 (2020) 115862. https://doi.org/10.1016/j.watres.2020.115862.

[30] J. Ali, A. Shahzad, J. Wang, J. Ifthikar, W. Lei, G.G. Aregay, Z. Chen, Z. Chen, Modulating the redox cycles of homogenous Fe(III)/PMS system through constructing electron rich thiomolybdate centres in confined layered double hydroxides, Chem. Eng. J. 408 (2021) 127242. https://doi.org/10.1016/j.cej.2020.127242.

[31] M. Pavlovic, R. Huber, M. Adok-Sipiczki, C. Nardin, I. Szilagyi, Ion specific effects on the stability of layered double hydroxide colloids, Soft Matter. 12 (2016) 4024–4033. https://doi.org/10.1039/C5SM03023D.

[32] Z.P. Xu, Y. Jin, S. Liu, Z.P. Hao, G.Q.M. Lu, Surface charging of layered double hydroxides during dynamic interactions of anions at the interfaces, J. Colloid Interface Sci. 326 (2008) 522–529. https://doi.org/10.1016/j.jcis.2008.06.062.

[33] Z. Somosi, S. Muráth, P. Nagy, D. Sebők, I. Szilagyi, G. Douglas, Contaminant removal by efficient separation of in situ formed layered double hydroxide compounds from

mine wastewaters, Environ. Sci. Water Res. Technol. 5 (2019) 2251–2259. https://doi.org/10.1039/C9EW00808J.

[34]   J. Matusik, J. Hyla, P. Maziarz, K. Rybka, T. Leiviskä, Performance of Halloysite-Mg/Al LDH Materials for Aqueous As(V) and Cr(VI) Removal, Materials. 12 (2019) 3569. https://doi.org/10.3390/ma12213569.

[35]   P. Hu, Y. Zhang, F. Lv, W. Tong, H. Xin, Z. Meng, X. Wang, P.K. Chu, Preparation of layered double hydroxides using boron mud and red mud industrial wastes and adsorption mechanism to phosphate, Water Environ. J. 31 (2017) 145–157. https://doi.org/10.1111/wej.12212.

[36]   A. Golban, L. Lupa, L. Cocheci, R. Pode, Synthesis of MgFe Layered Double Hydroxide from Iron-Containing Acidic Residual Solution and Its Adsorption Performance, Crystals. 9 (2019) 514. https://doi.org/10.3390/cryst9100514.

[37]   Z. Tang, Z. Qiu, S. Lu, X. Shi, Functionalized layered double hydroxide applied to heavy metal ions absorption: A review, Nanotechnol. Rev. 9 (2020) 800–819. https://doi.org/10.1515/ntrev-2020-0065.

[38]   E. Hiller, B. Lalinská, M. Chovan, Ľ. Jurkovič, T. Klimko, M. Jankulár, R. Hovorič, P. Šottník, R. Fľaková, Z. Ženišová, I. Ondrejková, Arsenic and antimony contamination of waters, stream sediments and soils in the vicinity of abandoned antimony mines in the Western Carpathians, Slovakia, Appl. Geochem. 27 (2012) 598–614. https://doi.org/10.1016/j.apgeochem.2011.12.005.

[39]   J. Majzlan, M. Števko, T. Lánczos, Soluble secondary minerals of antimony in Pezinok and Kremnica (Slovakia) and the question of mobility or immobility of antimony in mine waters, Environ. Chem. 13 (2016) 927. https://doi.org/10.1071/EN16013.

[40]   R. Fľaková, Z. Ženišová, D. Krčmář, I. Ondrejková, O. Sracek, OCCURRENCE OF ANTIMONY AND ARSENIC AT MINING SITES IN SLOVAKIA: IMPLICATIONS FOR THEIR MOBILITY, (n.d.) 9.

[41]   P. Sekula, E. Hiller, P. Šottník, Ľ. Jurkovič, T. Klimko, J. Vozár, Removal of antimony and arsenic from circum-neutral mine drainage in Poproč, Slovakia: a field treatment system using low-cost iron-based material, Environ. Earth Sci. 77 (2018) 518. https://doi.org/10.1007/s12665-018-7700-3.

[42]   H. Lu, Z. Zhu, H. Zhang, J. Zhu, Y. Qiu, Simultaneous removal of arsenate and antimonate in simulated and practical water samples by adsorption onto Zn/Fe layered double hydroxide, Chem. Eng. J. 276 (2015) 365–375. https://doi.org/10.1016/j.cej.2015.04.095.

[43]   J. Wang, T. Zhang, M. Li, Y. Yang, P. Lu, P. Ning, Q. Wang, Arsenic removal from water/wastewater using layered double hydroxide derived adsorbents, a critical review, RSC Adv. 8 (2018) 22694–22709. https://doi.org/10.1039/C8RA03647K.

[44]   K.-H. Goh, T.-T. Lim, Z. Dong, Application of layered double hydroxides for removal of oxyanions: A review, Water Res. 42 (2008) 1343–1368. https://doi.org/10.1016/j.watres.2007.10.043.

[45]   X. Liang, Y. Zang, Y. Xu, X. Tan, W. Hou, L. Wang, Y. Sun, Sorption of metal cations on layered double hydroxides, Colloids Surf. Physicochem. Eng. Asp. 433 (2013) 122–131. https://doi.org/10.1016/j.colsurfa.2013.05.006.

[46]   J.-Q. Jiang, S.M. Ashekuzzaman, J.S.J. Hargreaves, A.R. McFarlane, A.B.M. Badruzzaman, M.H. Tarek, Removal of Arsenic (III) from groundwater applying a reusable Mg-Fe-Cl layered double hydroxide, J. Chem. Technol. Biotechnol. 90 (2015) 1160–1166. https://doi.org/10.1002/jctb.4607.

[47]   B. Hudcová, M. Erben, M. Vítková, M. Komárek, Antimonate adsorption onto Mg-Fe layered double hydroxides in aqueous solutions at different pH values: Coupling surface

complexation modeling with solid-state analyses, Chemosphere. 229 (2019) 236–246. https://doi.org/10.1016/j.chemosphere.2019.05.008.

[48]   J. Brynda, S. Skoblia, M. Pohořelý, Z. Beňo, K. Soukup, M. Jeremiáš, J. Moško, B. Zach, L. Trakal, M. Šyc, K. Svoboda, Wood chips gasification in a fixed-bed multi-stage gasifier for decentralized high-efficiency CHP and biochar production: Long-term commercial operation, Fuel. 281 (2020) 118637. https://doi.org/10.1016/j.fuel.2020.118637.

[49]   Y. Seida, Y. Nakano, Y. Nakamura, Rapid removal of dilute lead from water by Pyroaurite-like compound, Water Res. 35 (2001) 2341–2346. https://doi.org/10.1016/S0043-1354(00)00523-6.

[50]   A.-M. Flank, G. Cauchon, P. Lagarde, S. Bac, M. Janousch, R. Wetter, J.-M. Dubuisson, M. Idir, F. Langlois, T. Moreno, D. Vantelon, LUCIA, a microfocus soft XAS beamline, Nucl. Instrum. Methods Phys. Res. Sect. B Beam Interact. Mater. At. 246 (2006) 269–274. https://doi.org/10.1016/j.nimb.2005.12.007.

[51]   D. Vantelon, N. Trcera, D. Roy, T. Moreno, D. Mailly, S. Guilet, E. Metchalkov, F. Delmotte, B. Lassalle, P. Lagarde, A.-M. Flank, The LUCIA beamline at SOLEIL, J. Synchrotron Radiat. 23 (2016) 635–640. https://doi.org/10.1107/S1600577516000746.

[52]   P.L. Smedley, D.G. Kinniburgh, A review of the source, behaviour and distribution of arsenic in natural waters, Appl. Geochem. 17 (2002) 517–568. https://doi.org/10.1016/S0883-2927(02)00018-5.

[53]   M. Filella, N. Belzile, Y.-W. Chen, Antimony in the environment: a review focused on natural waters II. Relevant solution chemistry, (2002) 21.

[54]   R. Flakova, Z. Zenisova, O. Sracek, D. Krcmar, I. Ondrejkova, M. Chovan, B. Lalinská, M. Fendekova, The behavior of arsenic and antimony at Pezinok mining site, southwestern part of the Slovak Republic, Environ. Earth Sci. 66 (2012) 1043–1057. https://doi.org/10.1007/s12665-011-1310-7.

[55]   P.Y.R. Suzaki, M.T. Munaro, C.C. Triques, S.J. Kleinübing, M.R. Fagundes Klen, R. Bergamasco, L.M. de Matos Jorge, Phenomenological mathematical modeling of heavy metal biosorption in fixed-bed columns, Chem. Eng. J. 326 (2017) 389–400. https://doi.org/10.1016/j.cej.2017.05.157.

[56]   S. Jaśkaniec, C. Hobbs, A. Seral-Ascaso, J. Coelho, M.P. Browne, D. Tyndall, T. Sasaki, V. Nicolosi, Low-temperature synthesis and investigation into the formation mechanism of high quality Ni-Fe layered double hydroxides hexagonal platelets, Sci. Rep. 8 (2018) 4179. https://doi.org/10.1038/s41598-018-22630-0.

[57]   X. Guo, Z. Wu, M. He, X. Meng, X. Jin, N. Qiu, J. Zhang, Adsorption of antimony onto iron oxyhydroxides: Adsorption behavior and surface structure, J. Hazard. Mater. 276 (2014) 339–345. https://doi.org/10.1016/j.jhazmat.2014.05.025.

[58]   I. Herath, M. Vithanage, J. Bundschuh, Antimony as a global dilemma: Geochemistry, mobility, fate and transport, Environ. Pollut. 223 (2017) 545–559. https://doi.org/10.1016/j.envpol.2017.01.057.

[59]   C. Hinz, Description of sorption data with isotherm equations, Geoderma. 99 (2001) 225–243. https://doi.org/10.1016/S0016-7061(00)00071-9.

[60]   Bioprocess Engineering Principles, Elsevier, 2013. https://doi.org/10.1016/C2009-0-22348-8.

[61]   I. Ondrejková, Z. Ženišová, R. Fľaková, D. Krčmář, O. Sracek, The Distribution of Antimony and Arsenic in Waters of the Dúbrava Abandoned Mine Site, Slovak Republic, Mine Water Environ. 32 (2013) 207–221. https://doi.org/10.1007/s10230-013-0229-5.

[62]   P. Qi, T. Pichler, Competitive adsorption of As(III), As(V), Sb(III) and Sb(V) onto ferrihydrite in multi-component systems: Implications for mobility and distribution, J. Hazard. Mater. 330 (2017) 142–148. https://doi.org/10.1016/j.jhazmat.2017.02.016.

[63] M. Avila, T. Burks, F. Akhtar, M. Göthelid, P.C. Lansåker, M.S. Toprak, M. Muhammed, A. Uheida, Surface functionalized nanofibers for the removal of chromium(VI) from aqueous solutions, Chem. Eng. J. 245 (2014) 201–209. https://doi.org/10.1016/j.cej.2014.02.034.

[64] T. Kameda, E. Kondo, T. Yoshioka, Equilibrium and kinetics studies on As(V) and Sb(V) removal by Fe2+-doped Mg–Al layered double hydroxides, J. Environ. Manage. 151 (2015) 303–309. https://doi.org/10.1016/j.jenvman.2014.12.050.

[65] S. Wang, B. Gao, Y. Li, Enhanced arsenic removal by biochar modified with nickel (Ni) and manganese (Mn) oxyhydroxides, J. Ind. Eng. Chem. 37 (2016) 361–365. https://doi.org/10.1016/j.jiec.2016.03.048.

[66] S. Wang, B. Gao, Y. Li, A.R. Zimmerman, X. Cao, Sorption of arsenic onto Ni/Fe layered double hydroxide (LDH)-biochar composites, RSC Adv. 6 (2016) 17792–17799. https://doi.org/10.1039/C5RA17490B.

[67] G.A. Waychunas, C.C. Fuller, B.A. Rea, J.A. Davis, Wide angle X-ray scattering (WAXS) study of "two-line" ferrihydrite structure: Effect of arsenate sorption and counterion variation and comparison with EXAFS results, Geochim. Cosmochim. Acta. 60 (1996) 1765–1781. https://doi.org/10.1016/0016-7037(96)89830-9.

[68] M.L. Farquhar, J.M. Charnock, F.R. Livens, D.J. Vaughan, Mechanisms of Arsenic Uptake from Aqueous Solution by Interaction with Goethite, Lepidocrocite, Mackinawite, and Pyrite: An X-ray Absorption Spectroscopy Study, Environ. Sci. Technol. 36 (2002) 1757–1762. https://doi.org/10.1021/es010216g.

[69] D. Wu, S.-P. Sun, M. He, Z. Wu, J. Xiao, X.D. Chen, W.D. Wu, As(V) and Sb(V) co-adsorption onto ferrihydrite: synergistic effect of Sb(V) on As(V) under competitive conditions, Environ. Sci. Pollut. Res. 25 (2018) 14585–14594. https://doi.org/10.1007/s11356-018-1488-2.

[70]   D. Mohan, C.U. Pittman, Activated carbons and low cost adsorbents for remediation of tri- and hexavalent chromium from water, J. Hazard. Mater. 137 (2006) 762–811. https://doi.org/10.1016/j.jhazmat.2006.06.060.

[71]   K.Y. Foo, B.H. Hameed, Insights into the modeling of adsorption isotherm systems, Chem. Eng. J. 156 (2010) 2–10. https://doi.org/10.1016/j.cej.2009.09.013.

[72]   I.L. Calugaru, C.M. Neculita, T. Genty, G.J. Zagury, Removal efficiency of As(V) and Sb(III) in contaminated neutral drainage by Fe-loaded biochar, Environ. Sci. Pollut. Res. 26 (2019) 9322–9332. https://doi.org/10.1007/s11356-019-04381-1.

[73]   F.L. Braghiroli, I.L. Calugaru, C. Gonzalez-Merchan, C.M. Neculita, H. Bouafif, A. Koubaa, Efficiency of eight modified materials for As(V) removal from synthetic and real mine effluents, Miner. Eng. 151 (2020) 106310. https://doi.org/10.1016/j.mineng.2020.106310.

[74]   M. Hassan, R. Naidu, J. Du, Y. Liu, F. Qi, Critical review of magnetic biosorbents: Their preparation, application, and regeneration for wastewater treatment, Sci. Total Environ. 702 (2020) 134893. https://doi.org/10.1016/j.scitotenv.2019.134893.

[75]   S. Bakshi, C. Banik, S.J. Rathke, D.A. Laird, Arsenic sorption on zero-valent iron-biochar complexes, Water Res. 137 (2018) 153–163. https://doi.org/10.1016/j.watres.2018.03.021.

[76]   R. He, Z. Peng, H. Lyu, H. Huang, Q. Nan, J. Tang, Synthesis and characterization of an iron-impregnated biochar for aqueous arsenic removal, Sci. Total Environ. 612 (2018) 1177–1186. https://doi.org/10.1016/j.scitotenv.2017.09.016.

[77]   X. Hu, Z. Ding, A.R. Zimmerman, S. Wang, B. Gao, Batch and column sorption of arsenic onto iron-impregnated biochar synthesized through hydrolysis, Water Res. 68 (2015) 206–216. https://doi.org/10.1016/j.watres.2014.10.009.

[78] M. Zhang, B. Gao, S. Varnoosfaderani, A. Hebard, Y. Yao, M. Inyang, Preparation and characterization of a novel magnetic biochar for arsenic removal, Bioresour. Technol. 130 (2013) 457–462. https://doi.org/10.1016/j.biortech.2012.11.132.

[79] S. Wang, B. Gao, Y. Li, Y. Wan, A.E. Creamer, Sorption of arsenate onto magnetic iron–manganese (Fe–Mn) biochar composites, RSC Adv. 5 (2015) 67971–67978. https://doi.org/10.1039/C5RA12137J.

[80] M. Williams, Arsenic in mine waters: an international study, Environ. Geol. 40 (2001) 267–278. https://doi.org/10.1007/s002540000162.

[81] Z. Wen, J. Xi, J. Lu, Y. Zhang, G. Cheng, Y. Zhang, R. Chen, Porous biochar-supported MnFe2O4 magnetic nanocomposite as an excellent adsorbent for simultaneous and effective removal of organic/inorganic arsenic from water, J. Hazard. Mater. 411 (2021) 124909. https://doi.org/10.1016/j.jhazmat.2020.124909.

[82] J.-P. Zou, H.-L. Liu, J. Luo, Q.-J. Xing, H.-M. Du, X.-H. Jiang, X.-B. Luo, S.-L. Luo, S.L. Suib, Three-Dimensional Reduced Graphene Oxide Coupled with Mn3O4 for Highly Efficient Removal of Sb(III) and Sb(V) from Water, ACS Appl. Mater. Interfaces. 8 (2016) 18140–18149. https://doi.org/10.1021/acsami.6b05895.

[83] M.A. Rahman, M.M. Rahman, M.M. Bahar, P. Sanderson, D. Lamb, Antimonate sequestration from aqueous solution using zirconium, iron and zirconium-iron modified biochars, Sci. Rep. 11 (2021) 8113. https://doi.org/10.1038/s41598-021-86978-6.

[84] H.U. Sø, D. Postma, R. Jakobsen, F. Larsen, Sorption and desorption of arsenate and arsenite on calcite, Geochim. Cosmochim. Acta. 72 (2008) 5871–5884. https://doi.org/10.1016/j.gca.2008.09.023.

[85] F. Renard, C.V. Putnis, G. Montes-Hernandez, H.E. King, G.D. Breedveld, G. Okkenhaug, Sequestration of Antimony on Calcite Observed by Time-Resolved Nanoscale Imaging, Environ. Sci. Technol. 52 (2018) 107–113. https://doi.org/10.1021/acs.est.7b04727.

[86]   S. Qiu, L. Yan, C. Jing, Simultaneous removal of arsenic and antimony from mining wastewater using granular TiO2: Batch and field column studies, J. Environ. Sci. 75 (2019) 269–276. https://doi.org/10.1016/j.jes.2018.04.001.

[87]   H. Zeng, M. Arashiro, D.E. Giammar, Effects of water chemistry and flow rate on arsenate removal by adsorption to an iron oxide-based sorbent, Water Res. 42 (2008) 4629–4636. https://doi.org/10.1016/j.watres.2008.08.014.

[88]   G. Ungureanu, S.C.R. Santos, I. Volf, R.A.R. Boaventura, C.M.S. Botelho, Biosorption of antimony oxyanions by brown seaweeds: Batch and column studies, J. Environ. Chem. Eng. 5 (2017) 3463–3471. https://doi.org/10.1016/j.jece.2017.07.005.

[89]   L. Li, H. Tu, S. Zhang, L. Wu, M. Wu, Y. Tang, P. Wu, Geochemical behaviors of antimony in mining-affected water environment (Southwest China), Environ. Geochem. Health. 41 (2019) 2397–2411. https://doi.org/10.1007/s10653-019-00285-8.

[90]   S.G. Johnston, W.W. Bennett, N. Doriean, K. Hockmann, N. Karimian, E.D. Burton, Antimony and arsenic speciation, redox-cycling and contrasting mobility in a mining-impacted river system, Sci. Total Environ. 710 (2020) 136354. https://doi.org/10.1016/j.scitotenv.2019.136354.

[91]   J. Majzlan, B. Lalinská, M. Chovan, L. Jurkovič, S. Milovská, J. Göttlicher, The formation, structure, and ageing of As-rich hydrous ferric oxide at the abandoned Sb deposit Pezinok (Slovakia), Geochim. Cosmochim. Acta. 71 (2007) 4206–4220. https://doi.org/10.1016/j.gca.2007.06.053.

[92]   M. Filella, S. Philippo, N. Belzile, Y. Chen, F. Quentel, Natural attenuation processes applying to antimony: a study in the abandoned antimony mine in Goesdorf, Luxembourg, Sci. Total Environ. 407 (2009) 6205–6216. https://doi.org/10.1016/j.scitotenv.2009.08.027.
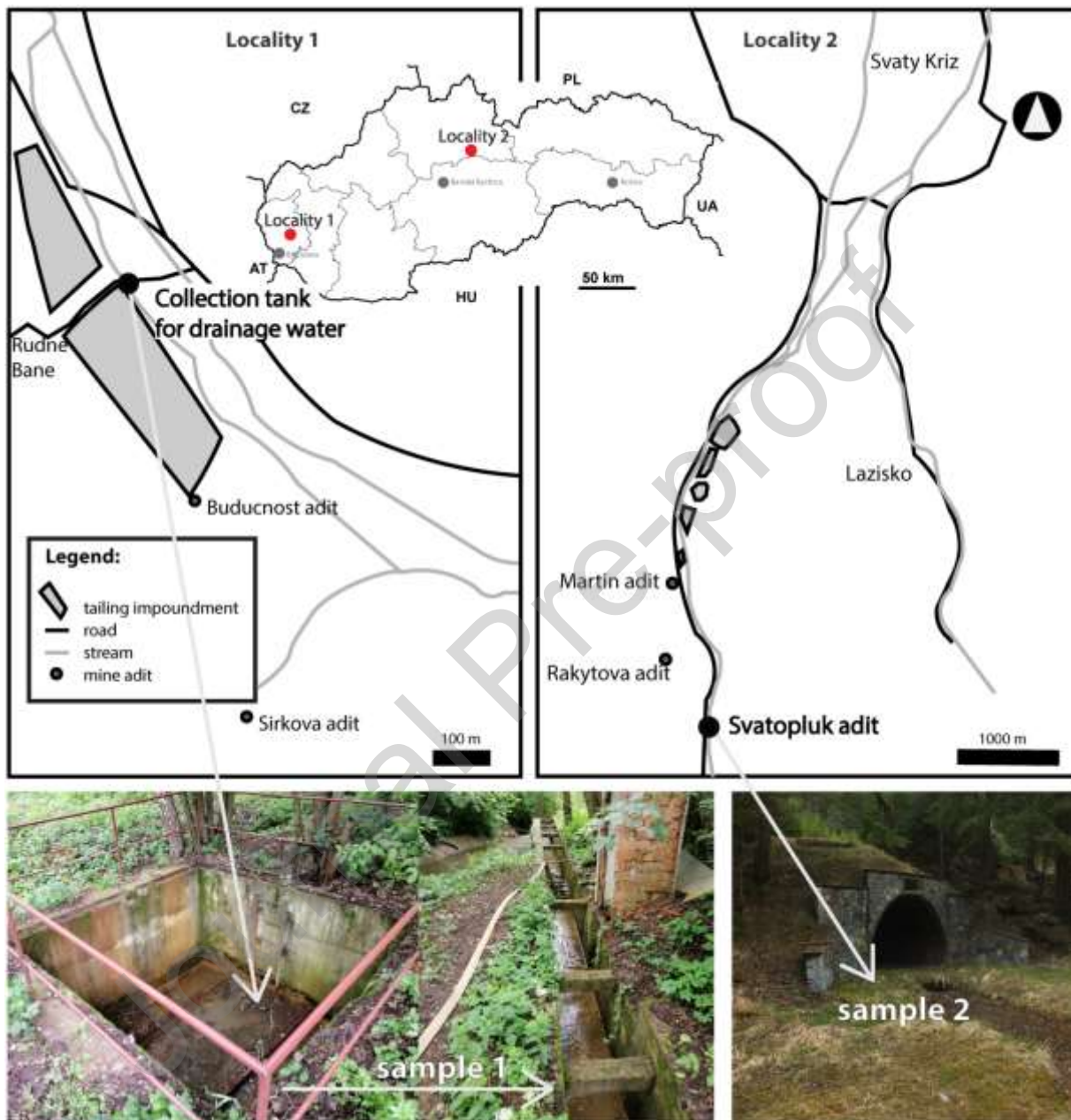
List of Figures:

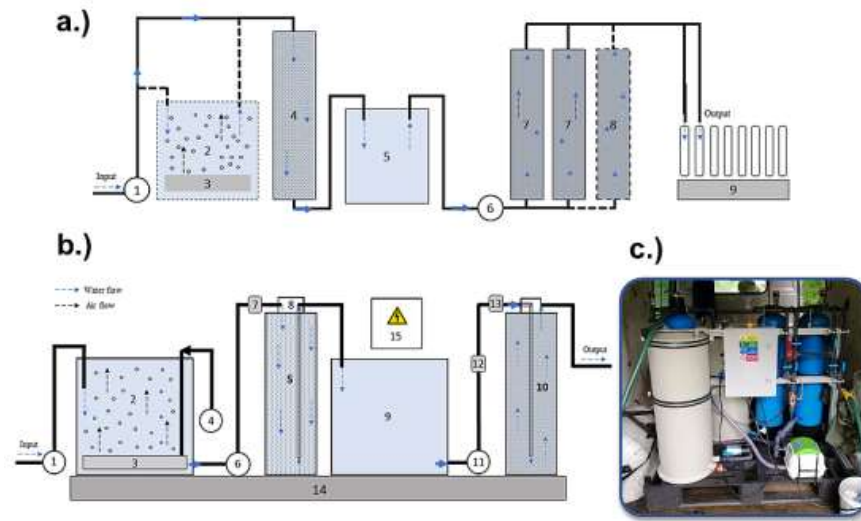**Figure 1:** Mine water sampling sites.

igure 2: The small-scale (solid line) and large-scale (solid and/or dashed line) laboratory column experiment (**a**): peristaltic pumps (1, 6) aeration tank (2) air blower (3) filtration column (4) storage tank (5) adsorption columns (7, 8) collector (9). The field scale column technology (**b**): peristaltic pumps (1, 6, 11) aeration tank (2) aeration element with air blower (3, 4) filtration column (5) barometers (7, 13) valve (8) storage tank (9) adsorption column (10) flowmeter (12) mobile platform (14) electricity supply (15). A mobile double-column set-up (**c**).
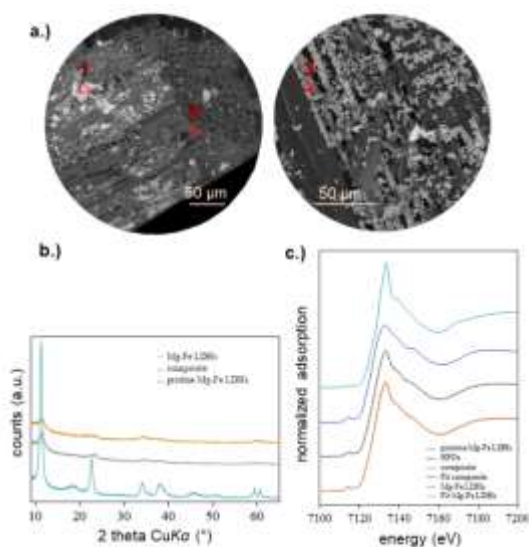
Figure 3: BSE images (**a**), XRD patterns (**b**) and Fe *K*-XANES patterns (**c**) of the composite. Mg-Fe LDHs from Fe-rich sludge (1); biochar (2); carbonates formed after the field application of the composite (3). HFOs and pristine Mg-Fe LDHs were used as references for Linear Combination Fits.
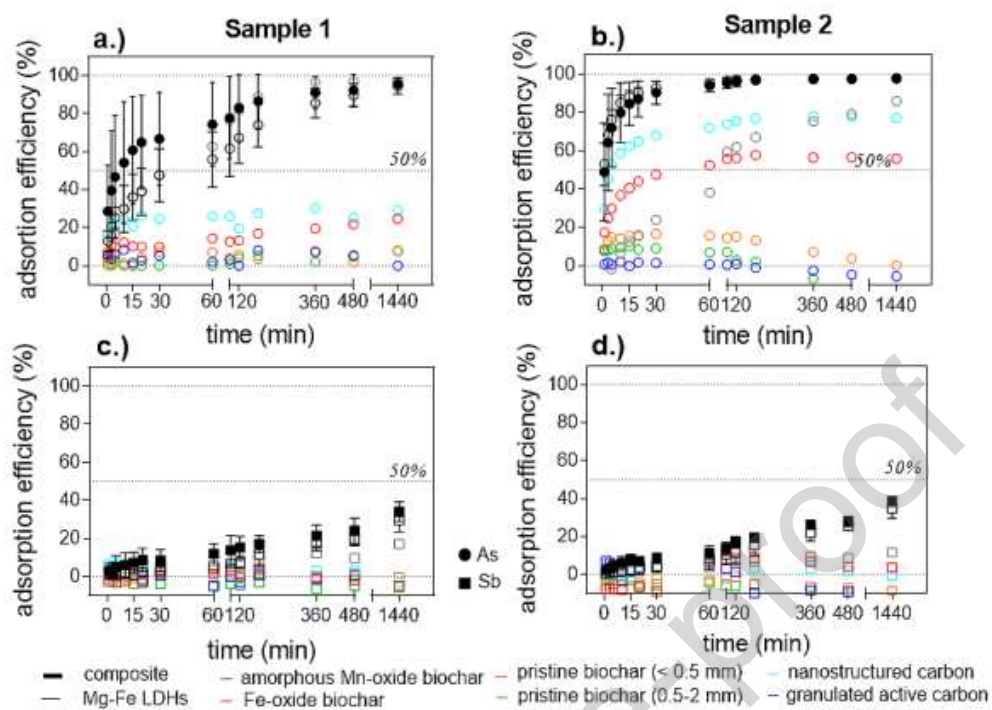
Figure 4: As(V) (**a, b**) and Sb(V) (**c, d**) adsorption kinetics in mine waters (error bars represent standard deviation of the average for the composite and Mg-Fe LDHs). Comparison with pristine and modified biochar, and with commercially used materials for water treatment.
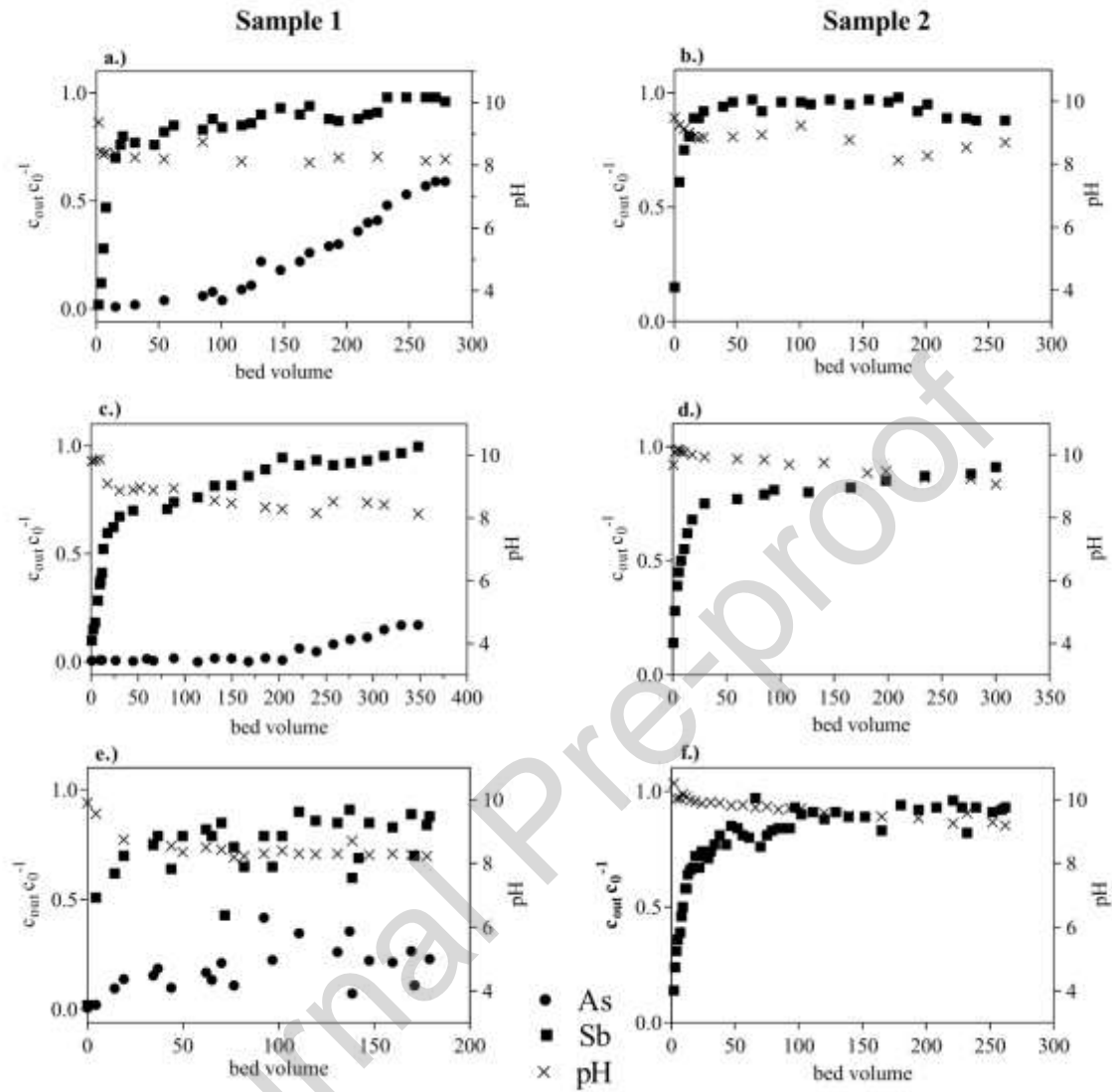
Figure 5: Breakthrough curves in a small, large, and field scale, respectivelly on sample 1 (**a, c, e**) and sample 2 (**b, d, f**).
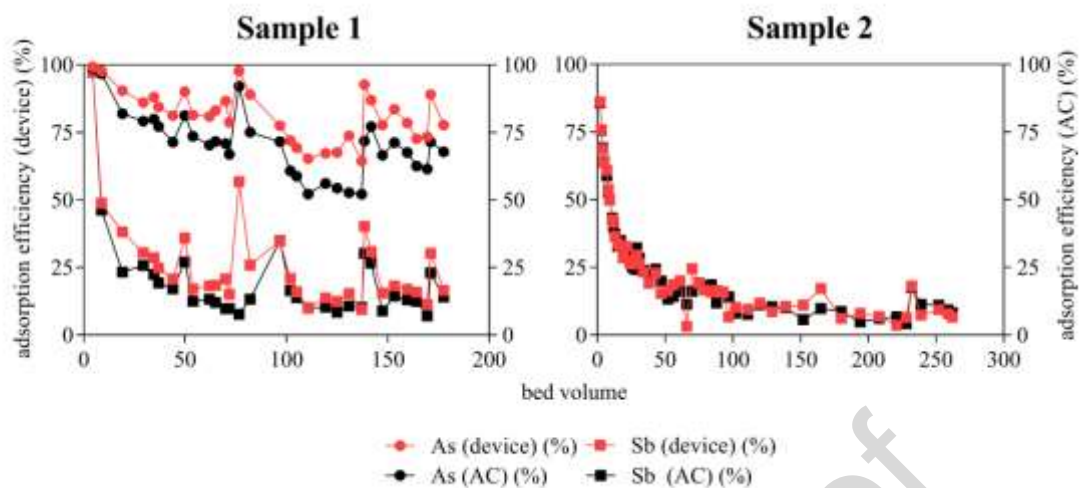
Figure 6: Comparison of the adsorption efficiency (%) of the whole technological column device with the adsorption column (AC) for As(V) and Sb(V).

Table 1: Feedstocks and characteristics of the composite.

	Laboratory Condition	Pilot Plant Condition
Input Reactants		
Dilluted Fe-leachate (1:1) (mL)	200	4000
$MgCl_2 \times 6H_2O$ (g)	30.5	609.8
Biochar (g)	12.5	250
2.5 M KOH (mL)	400	8 000
Yield of composite (g)	35	700
Composite		
Biochar fraction (mm)	< 0.5	0.5 - 2
S_{BET} ($m^2\ g^{-1}$)	274	215
S_{meso} ($m^2\ g^{-1}$)	209	130
V_{tot} ($mm^3{}_{liq}\ g^{-1}$)	274	271
V_{micro} ($mm^3{}_{liq}\ g^{-1}$)	37	46
CEC^* ($cmol^+ kg^{-1}$)	113.5 ± 0.9	152.4 ± 8.4
pH_{H2O}**	9.9 ± 0.03	10.5 ± 0.008
pH_{PZC}	10.1	10.4
Fe_{TOT} ($g\ kg^{-1}$)	205.2	247.2
Mg_{TOT} ($g\ kg^{-1}$)	76.0	78.6
K_{TOT} ($g\ kg^{-1}$)	13.1	24.8
Ca_{TOT} ($g\ kg^{-1}$)	8.3	6.5
Mn_{TOT} ($g\ kg^{-1}$)	2.4	1.8
Al_{TOT} ($g\ kg^{-1}$)	1.4	1.4

* CEC (± SD) could be overestimated by releasing K and Mg from the composite.

** Presented as average ± SD.

Table 2: Parameters of the laboratory and field scale column experiments.

Parameter	Small Lab. Scale		Large Lab. Scale		Field Scale	
	Sample 1	Sample 2	Sample 1	Sample 2	Sample 1	Sample 2
Composite (g)	1	2	21	21	2 000	2 000
Quartz sand (g)	9	18	317	317	30 000	30 000
Composite/sand ratio	1:9	1:9	1:15	1:15	1:15	1:15
Flow rate (mL min^{1-}; L hod^{-1} for field scale)	2	2	20	20	85-138	89-93
Adsorption bed high (cm)	8	11	19.7	19.7	75	75
Adsorption bed width (cm)	1	2	4.2	4.2	19	19
Bed volume	279	263	348	300	179	262
Aeration pre-treatment	no	no	yes	yes	yes	yes
Mine water total volume (L)	8.64	8.16	96.4	83.1	3 936	5 757

Table 3: A comparison of the adsorbed amount (Q_{max}) of As(V) and Sb(V) on different LDH-

and Fe-based biochar composites.

	LDHs or Fe-based materials	Origin of biochar	Q_{max} (mg g^{-1})	Reference
As (V)	Mg-Fe LDH/HFO	Wood	**21.0**	This study
	Ni/Mn LDH	Pine wood	6.52	[56]
	Ni/Fe LDH	Pine wood	4.38	[57]
	Cu/Al LDH	Corn stalk	14.9	[33]
	Zn/Al LDH	Corn stalk	16.1	[33]
	Mg/Al LDH	Corn stalk	10.4	[33]
	Zero valent iron	Red oak	15.6	[66]
	Zero valent iron	Switchgrass	7.92	[66]
	FeCl$_3$	Corn straw	6.80	[67]
	FeCl$_3$	Wood ash	5.78	[63]
	Goethite	Hickory chips	2.16	[68]
	Maghemite	Cottonwood	3.15	[69]
	Fe-Mn oxide	Pine wood	3.44	[70]
Sb (V)	Mg-Fe LDH/HFO	Wood	**25.0**	This study
	Fe oxide	Biosolid	39.7	[71]
	FeCl$_3$	Biosolid	31.5	[71]

CRediT authorship contribution statement

Veronika Veselská: Conceptualization, draft writing and editing, revising the manuscript, management of composite synthesis, performing batch laboratory experiments and field application.

Hana Šillerová: Design and performing of the column experiments, conducting of the equilibrium batch experiments, draft writing, results discussion.

Barbora Hudcová: Design of composite synthesis, interpretation of the kinetic batch experiments, draft writing.

Gildas Ratié: XAS results interpretation and deep result discussion and commenting on the manuscript.

Petr Lacina: Design of mobile double-column technology, field application, results discussion.

Bronislava Lalinská-Voleková: Field application, description of the localities.

Lukáš Trakal: Biochar modification, field application, commenting on the manuscript.

Peter Šottník: Mine water samples characterization, field application.

Ľubomír Jurkovič: Field application, results discussion.

Michael Pohořelý: Composite synthesis in pilot plant conditions.

Delphine Vantelon: XAS measurements at LUCIA beamline, results discussion.

Ivo Šafařík: Biochar modification.

Michael Komárek: Discussion and commenting on the manuscript.

Declaration of interests

☒ The authors declare that they have no known competing financial interests or personal relationships that could have appeared to influence the work reported in this paper.

☐The authors declare the following financial interests/personal relationships which may be considered as potential competing interests:

Highlights:

- The composite was prepared from Fe-rich sludge and certified woody biochar.

- Efficient As and Sb removal in batch and continuous flow column systems.

- Successful field application of the composite for local mine water treatment.

- Continues flow columns are complementary to passive geochemical barriers.